Journal of Biological Engineering

RESEARCH

Open Access

# Efflux pump knockout minimizes crosstalk and boosts response in transcription factor-based biosensors

Jinju Lee[1,3†], Byeong-hyeon Yoo[1,3†], Eunjung Jeon[1], Haram Kong[1], Eugene Rha[1], Jonghyeok Shin[1,2,3], Hyewon Lee[1,2,3], Haseong Kim[1,2,3,4], Dae-Hee Lee[1,2,3,4,5], Kil Koang Kwon[1,2,3*] and Seung-Goo Lee[1,2,3,4*]

## Abstract

**Background** Cellular transport systems are key determinants of intracellular molecule concentrations and can be utilized to modulate the responsiveness of transcription factor (TF)-based biosensors. Efflux pumps facilitate the export of small molecules; therefore, their activity can directly compromise the accuracy of biosensor-based assays. We engineered a cellular export machinery to enhance the responsiveness and reduce crosstalk of a DmpR-based biosensor, which employs the phenol-responsive TF DmpR to detect intracellular phenolic ligands but is affected by ligand diffusion between cells. To overcome this limitation, efflux pump genes were knocked out to minimize ligand diffusion and improve signal fidelity.

**Results** Among the efflux pumps tested, deletion of *mdtA* was found to promote effective intracellular accumulation of phenolic compounds. This strategy not only increased biosensor sensitivity by up to 19-fold but also reduced false positives during enzyme screening by suppressing intercellular diffusion of enzymatic products. In the mock library experiment, the proportion of false positives relative to the total positive cells was 74% in the wild-type strain, whereas it was only 5% in the Δ*mdtA* strain. To demonstrate the applicability of this approach to an enzyme screening platform, we targeted penicillin G acylase (PGA), an enzyme useful for producing semi-synthetic antibiotics. Knockout of *mdtA* effectively reduced false positives during flow cytometry-based high-throughput screening. Using this biosensor platform, several PGA variants with improved catalytic activity were successfully identified from a random mutagenesis library.

**Conclusions** Overall, host engineering to adjust cellular conditions and ligand concentrations provides a versatile approach to enhance the sensitivity, precision, and efficiency of single-cell-based enzyme screening platforms.

**Keywords** Transcription factor-based biosensor, Efflux pump, High-throughput screening, Penicillin G acylase, Enzyme engineering

†Jinju Lee and Byeong-hyeon Yoo are contributed equally to this work.

*Correspondence:
Kil Koang Kwon
kkkwon@kribb.re.kr
Seung-Goo Lee
sglee@kribb.re.kr

Full list of author information is available at the end of the article

## Background

Microorganisms possess systems that expel harmful substances from the cell to ensure survival and adaptation to various environments [1, 2]. Among these systems, efflux pumps transport intracellular compounds, such as antibiotics, detergents, phenolic compounds, and free fatty acids, to the periplasm or extracellular space [3–6]. These transporters contribute to maintaining cellular homeostasis and are involved in intracellular detoxification [7, 8]. Notably, deletion of efflux pump genes responsible for substrate recognition can lead to a significant increase in antibiotic susceptibility, highlighting their physiological importance [9–12]. For example, modulation of pump expression can reduce the minimum inhibitory concentration of tetracycline by up to 100-fold [13].

Given their critical role in regulating the intracellular concentrations of various compounds, efflux pumps can serve as attractive targets for enhancing the performance of TF-based biosensors that respond to internal ligands [14]. While most TF-based biosensor optimization approaches have focused on tuning genetic components, such as promoters, TFs, and reporters [15–17], host engineering provides an alternative strategy for independently modulating biosensor performance. Introducing or modulating membrane transport systems that facilitate the uptake of target ligands into the cell has emerged as an effective strategy to improve the sensitivity and responsiveness of TF-based biosensors [18–23].

Beyond improving sensitivity, efflux pump knockout also mitigates false positives, offering a critical advantage in single-cell biosensor applications [24, 25]. TF-based biosensors quantitatively detect enzymatic reactions that generate target ligands, enabling their broad application in high-throughput enzyme screening and engineering [26]. In producing cells, the generated ligands activate the biosensor circuit and lead to fluorescent protein expression, thereby linking enzymatic activity to a measurable output. However, because generated ligands are typically small molecules, they readily diffuse beyond the producing cells and spuriously activate biosensor circuits in neighboring non-producer cells [27]. Such unintended activation leads to false positives, a problem that becomes especially severe in large-scale library screening where only a minute fraction of variants represent true hits. In this context, even modest crosstalk can overwhelm the detection system, drastically reducing screening precision and efficiency. To address this critical limitation, we hypothesized that knocking out specific efflux pump genes would not only increase intracellular ligand concentration but also minimize intercellular ligand diffusion, thereby improving biosensor sensitivity and precision during enzyme screening.

In this study, we knocked out 21 efflux pumps in a previously established DmpR-based Genetic Enzyme Screening System (GESS), which employs DmpR as a TF to detect phenolic compounds generated by enzymatic reactions [26, 28–32]. As the transport of phenolic compounds is mediated by several efflux pumps in the genome [33], removing endogenous transporters from the host strain was expected to enhance signal resolution in DmpR-GESS. To evaluate this aspect, we tested three different enzymes—tyrosine phenol-lyase (E.C. 4.1.99.2, TPL) [28], penicillin G acylase (E.C. 3.5.1.11, PGA) [34], and cellulase (E.C. 3.2.1.4) [35]. Each enzyme, in combination with its corresponding substrate, generates a distinct phenolic product that can be detected by DmpR-GESS. Among these, PGA was chosen for in-depth analysis due to its industrial relevance in β-lactam antibiotic production [34, 36, 37]. To establish an efficient biosensor system, we employed this strategy to engineer PGA through flow cytometry-based single-cell screening.

## Methods

### Materials

All chemical reagents, except for *N*-(2-hydroxyphenyl)-2-phenylacetamide (HPPA), were purchased from Sigma-Aldrich (St. Louis, MO, USA). For plasmid construction, a plasmid DNA isolation kit (Cat No. CMP0112) and a DNA extraction kit (Cat. No. CMA0112) were purchased from Cosmo Genetech (Seoul, Korea). All oligonucleotides used in this study were synthesized by Macrogen (Daejeon, Korea) (Supplementary Table 1). Gibson assembly mix (Cat. No. E2611L) was purchased from New England Biolabs (Beverly, MA, USA). HPPA (Cat. No. BD701714) was purchased from BLD Pharmatech Ltd. (Shanghai, China) and dissolved primarily in dimethyl sulfoxide (DMSO, Sigma-Aldrich, Cat. No. D8418) to prepare a 0.1 M solution before use. The percentage of DMSO was limited to 2–5% in each reaction.

### Strains and plasmids

*Escherichia coli* BW25113 and its derivative strains from the KEIO collection were used as host strains for the biosensor system (Supplementary Table 2) [38]. Efflux pump-encoding gene knockout strains were selected from the EcoCyc database by retrieving proteins using the keyword 'efflux pump' [39]. The DmpR-GESS plasmid was constructed by substituting the pMB1-derived origin of pUC19 plasmid with the p15A origin and inserting a DmpR mutation (M52I) into mGESSv4 [28]. p15A-mGESSv4 (M52I) contained a genetic circuit composed of the activator-type TF DmpR, the $P_{DmpR}$ promoter derived from *Pseudomonas putida* KCTC1452, and *sfgfp* as the reporter [28]. The primers used to construct the plasmids for the experiments are listed in Supplementary Table 1. To integrate the DmpR-GESS (M52I) circuit into the *E. coli* BW25113 genome, the recombinant plasmid pKD46 was used. The kanamycin resistance gene

was subsequently eliminated using pCP20, resulting in a biosensor strain free of antibiotic resistance markers [26, 40].

For additional efflux pump expression, *mdtA*, *mdtG*, *emrE*, and *hsrA* were amplified by PCR using the BW25113 chromosome as a template and cloned into p15A-mGESSv4 (M52I) via Gibson assembly.

For enzyme expression, the following genes were cloned into plasmids: the TPL gene from *Citrobacter freundii* [41], a cellulase gene exhibiting bifunctional endo- and exo-cellulase activity [42], and PGA from *Escherichia coli*, which was cloned without its signal sequence to allow biosensor activation in the cytosol [43]. These genes were inserted into plasmids pHCEIIB-TPL [44], pCC1-CelEdx16 [35], and pSEVA234-llpac, respectively.

### Fluorescent analysis

Luria-Bertani (LB) medium (10 g/L tryptone, 5 g/L yeast extract, 10 g/L NaCl) and M9 minimal medium (12.8 g/L $Na_2HPO_4{\cdot}7H_2O$, 3 g/L $KH_2PO_4$, 0.5 g/L NaCl, 1 g/L $NH_4Cl$, 2 mM $MgSO_4$, 0.1 mM $CaCl_2$, 0.4% (w/v) acetate, and 0.01% (w/v) thiamine) were used with appropriate antibiotics as required. Ampicillin, kanamycin, and chloramphenicol were used at final concentrations of 100, 34, and 25 μg/mL, respectively.

To evaluate biosensor performance in response to ligand treatment, cells were cultured in LB medium at 37 ℃ until the optical density at 600 nm ($OD_{600}$) reached 1.5–3.0. Cells were then transferred to M9 medium supplemented with 4 g/L acetate for substrate treatment in a two-step reaction [32]. In this process, cells were first cultured with glucose as a carbon source and subsequently transferred to medium containing acetate, a non-preferred carbon source for *E. coli*, to promote $\sigma^{54}$–dependent transcription rather than cell growth. At the point of transfer, the cell OD was adjusted to 0.5 to ensure consistency across samples.

For the indirect assay of enzyme activity using the biosensor, cells were grown in LB medium at 37 ℃ and induced with 0.1 mM isopropyl β-D-1-thiogalactopyranoside (IPTG) at an $OD_{600}$ of 0.4, followed by incubation for an additional 6 h. After induction, cells were harvested by centrifugation at 1,000 ×*g* for 5 min and resuspended in M9 medium containing 4 g/L acetate. Phenolic compounds were added as ligands, and the cultures were incubated at 37 ℃ for 16 h prior to fluorescence measurement. DmpR M52I exhibited an increase in GFP signal after approximately 4 h and reached saturation around 12 h [45]; in this study, fluorescence signals were measured after saturation for the biosensor sensitivity experiments. Fluorescence intensity was measured using a fluorescence microplate reader (PerkinElmer, Waltham, MA, USA) with excitation and emission wavelengths of 485 nm and 535 nm, respectively. When analyzing the performance of the biosensor, fluorescence intensity was normalized to optical density to correct for potential OD variations among biological samples.

### Quantitative evaluation of whole-cell biosensor performance

The functional parameters of the whole-cell biosensors were evaluated. To establish the limit of blank (LOB), fluorescence signals from non-induced cells were collected across multiple independent replicates. The LOB was calculated as follows:

$$\mathrm{LOB} = \mu_{\,\mathrm{blank}} + 1.645 \times \delta_{\,\mathrm{blank}}$$

where $\mu_{blank}$ represents the mean fluorescence intensity of non-induced samples, and $\delta_{blank}$ is the standard deviation [46]. The z-score (1.645) was derived from a standard normal Gaussian distribution, and LOB represents 95% of the observed values.

For limit of detection (LOD) calculation, fluorescence intensities were measured across a range of each ligand concentration. The calculation was performed using the following equation:

$$\mathrm{LOD} = \mathrm{LOB} + 1.645 \times \delta_{\,\mathrm{low}}$$

where $\delta_{low}$ represents the standard deviation of fluorescence at the lowest ligand concentration.

Additionally, the signal-to-noise (S/N) ratio was calculated using the average fluorescence value measured at a given ligand concentration. The S/N ratio was calculated as follows:

$$\mathrm{S}/N\mathrm{ratio} = (\mu_{\,\mathrm{signal}} - \mu_{\,\mathrm{blank}})/\delta_{\,\mathrm{blank}}$$

where $\mu_{signal}$ represents the mean fluorescence intensity of the induced sample.

### Determination of phenolic compound concentrations

To measure the intracellular concentration of phenolic compounds, an overnight seed culture was inoculated at 1% (v/v) into 50 mL of LB medium. The culture was incubated at 37 ℃ until the $OD_{600}$ reached 1.0, followed by treatment with 100 μM phenolic compounds. At each sampling time point, cells were harvested by centrifugation at 1,000 ×*g* for 5 min and washed with an equal volume of phosphate-buffered saline (PBS). The resulting pellets were concentrated and resuspended in 1 mL of PBS, then subjected to sonication for 2 min to lyse the cells. Cell debris was removed by centrifugation at 22,000 ×*g* for 20 min. Phenolic compounds in the supernatant were extracted by adding an equal volume of ethyl acetate, followed by vortexing for 30 min.

To measure the extracellular concentration of phenolic compounds, cells were cultured in 1 mL of LB medium until the $OD_{600}$ reached 1.0, after which the culture supernatant was collected by centrifugation. An equal volume of ethyl acetate was added, and the mixture was vortexed and centrifuged to obtain the organic phase, which was subsequently subjected to HPLC analysis.

Reaction samples were analyzed using a liquid chromatograph (Agilent, Santa Clara, CA, USA) fitted with a ZORBAX Eclipse XDB-C18 column (4.6 × 150 mm; Agilent) at 270 nm. The mobile phase consisted of 0.1% [v/v] formic acid in water (buffer A) and acetonitrile (buffer B). The gradient program was as follows: 0–3 min, 80% A; 3–6 min, linear decrease from 80 to 70% A; 6–9 min, from 70 to 50% A; 9–12 min, from 50 to 30% A; 12–15 min, from 30 to 0% A; and 15–18 min, linear increase from 0 to 90% A. The flow rate was maintained at 0.7 mL/min throughout the run, and the column temperature was held at 25 ℃.

#### Mutant PGA library construction

A mutant PGA library was constructed using the Diversify PCR Random Mutagenesis Kit (Takara Bio, CA, USA) at a mutation frequency of approximately 2 mutations per kilobase and assembled with the pSEVA234 plasmid by Gibson assembly. The host strain used was *E. coli* BW25113, in which the DmpR-GESS (M52I) circuit was integrated into the chromosome [26]. The initial library constructed in *E. coli* DH5α yielded a library size of $7.2 \times 10^6$. The plasmids recovered from the library were re-transformed into the BW25113 strain, resulting in a library size of $1.2 \times 10^9$ colonies, exceeding the original library size by more than 100-fold.

#### Fluorescence-activated cell sorting (FACS) analysis

For FACS analysis, the biosensor host strain mGBW02, in which the DmpR-GESS (M52I) circuit was integrated into the *bglA* region of the *E. coli* BW25113 genome, was used. In experiments addressing the issue of false positives, positive cells were defined as those harboring both the target enzyme expression plasmid pSEVA234-llpac and the pACBB empty vector, while negative cells were defined as those carrying the pSEVA234 empty vector and the pACBB-tdTomato plasmid, which expresses the tdTomato fluorescent protein for visual identification. To evaluate the effect of efflux pump knockout, a mock library was constructed by mixing positive and negative cells at a 1:1 ratio.

Cells were cultured in LB medium with appropriate antibiotics. Cultures were incubated at 37 ℃ in a shaking incubator until the $OD_{600}$ reached 0.4, followed by induction with 0.1 mM IPTG for an additional 6 h. After IPTG induction, cells expressing the target enzyme were harvested by centrifugation at 1,000 ×*g* for 5 min and transferred to M9 medium containing 4 g/L acetate. During this transfer, 100 μM HPPA was added, and the cultures were incubated at 37 ℃ for up to 3 h. For FACS analysis, the cultured cells were diluted 1:100 in PBS. Flow cytometry was performed by measuring green (excitation: 488 nm) and red (excitation: 633 nm) fluorescence. The cell populations were gated based on the distributions of forward and side scatter to exclude cell debris and dead cells. Data were analyzed using BD CellQuest Pro (version 4.0.2, BD Biosciences, Franklin Lakes, NJ, USA) and FlowJo software (BD Biosciences, Franklin Lakes, NJ, USA). To determine the presence of green fluorescent protein (GFP) expression, the limit of quantitation (LOQ) was calculated based on the published literature [47].

Cells exhibiting high fluorescence intensity were sorted using FACSAriaIII instrument (BD Biosciences, NJ, USA). The library was inoculated in 10 mL of LB medium containing 12.5 μg/mL kanamycin and incubated at 37 ℃ for 3 h. For enzyme overexpression, 0.1 mM IPTG was added, and the culture was incubated at 23 ℃, 150 rpm overnight (18 h). The culture medium was changed to M9 containing 4 g/L acetate and 12.5 μg/mL kanamycin and adjusted to a final $OD_{600}$ of 0.5 prior to treatment with 100 μM HPPA. A blue laser (488 nm) and bandpass filter (530/30 nm) were used to analyze fluorescence intensity after 2 h of reaction. To minimize ligand diffusion that could occur over time, the reaction time for the false positive-related experiments was kept relatively short. In the first round of FACS screening, approximately 100,000 cells with high fluorescence intensity (top 3%) were collected and recovered in LB medium at 37 ℃ overnight. In the second and third rounds, 100,000 cells with top 1% fluorescence intensity were collected. Considering the environmental stress of the knockout strains, HPPA concentration was decreased to 50 μM in the third round. In the subsequent 96-well plate-based assay, a reaction time of 18 h was employed to clearly detect differences among the samples.

#### Kinetic analysis of PGA

For enzyme purification and kinetic analysis, the pSEVA234 plasmid harboring mutant enzymes was transformed into *E. coli* BL21. Cells were harvested by centrifugation and disrupted on ice by ultrasonication in 50 mM potassium phosphate buffer (pH 7.0). Intact cells and cell debris were removed by centrifugation at 16,600 ×*g* for 10 min at 4 ℃. The supernatants were filtered and applied to NGC Quest 10 (Bio-Rad, Hercules, CA, USA) equipped with an EconoFit Profinity IMAC column (Cat. #12009298, Bio-Rad). Purified proteins were quantified by the standard Bradford method [48]. The purified samples were analyzed by SDS-PAGE using a pre-stained ladder (Cat #1610374, Bio-Rad) as a reference. Expression of

the variants was analyzed using ImageJ (National Institutes of Health, Bethesda, MD, USA) and calculated by comparing band intensity with that of the housekeeping protein, glyceraldehyde 3-phosphate dehydrogenase (GAPDH).

Enzyme reactions were performed in 100 µL of potassium phosphate buffer (pH 7.0). The PGA activity assay was conducted at 40 ℃ using a thermomixer. High-performance liquid chromatograph (HPLC, Agilent, Santa Clara, CA, USA) was used to quantify phenylacetic acid, the enzymatic product of PGA. Reaction samples were analyzed using a liquid chromatograph (Agilent, Santa Clara, CA, USA) equipped with a ZORBAX Eclipse XDB-C18 column (4.6. × 150 mm; Agilent) at 215 nm. The mobile phase consisted of 0.1% [v/v] formic acid in water (buffer A) and acetonitrile (buffer B). The gradient program was as follows: 0–3 min, 99% A; 3–16.3 min, linear decrease from 99% to 45% A; 16.3–20 min, from 45 to 99% A. The injection volume was 5 µL for each sample. The flow rate was maintained at 1.0 mL/min throughout the run, and the column temperature was held at 25 ℃. Phenylacetic acid, the enzymatic product of PGA, has a retention time of 13.7 min. The concentration of the product was determined using a standard curve plotted with concentration versus peak area. Kinetic analysis was performed using nonlinear regression analysis in Prism 9 program (GraphPad, Boston, MA) based on data obtained from HPLC analysis.

### Computational simulation and structural analysis for mutant enzyme

Structural predictions of mutant enzymes selected through the fluorescence-based biosensor assay were conducted using the web-based AlphaFold 3 platform [49]. To analyze the effects of mutations on enzyme structural stability and interactions with the substrate, the software tools Discovery Studio and CB-Dock2 were employed. CB-Dock2 was used to predict ligand-binding cavities using both structure-based and template-based docking methods [50, 51]. The software identifies potential binding pockets and calculates binding scores based on the predicted interaction energies between the ligand and the protein.

When the mutant EcPGA structure was submitted to CB-Dock2, the server automatically selected the wild-type EcPGA structure complexed with SOX (a hydroxylated derivative of penicillin G) from the PDB ID 1GM9 as the docking template [52]. The predicted ligand-binding conformations were generated based on this template by an analysis tool FitDock, which is integrated in CB-Dock2 [53]. Interactions between the mutation site and surrounding residues were analyzed using Discovery Studio.

## Results

### Enhancing biosensor response by efflux pump deletion

In whole-cell biosensor systems designed to detect enzyme activity, enzymatic products generated by catalytic reactions bind to TFs to produce a measurable biological signal. Increasing the intracellular concentration of the ligand can enhance the effectiveness of such biosensors (Fig. 1). However, small molecules are not retained within the cell and may passively diffuse across the membrane or be actively exported via transporters [54]. To evaluate whether increasing intracellular ligand levels can enhance biosensor sensitivity, efflux pump knockout strains were selected from the KEIO collection (Supplementary Table 3) [38]. A total of 21 efflux pump knockout strains from the KEIO collection, which consists of *E. coli* BW25113 derivatives with single deletions of non-essential genes, were used as potential DmpR-GESS chassis. Although knockouts of certain genes could potentially affect cell growth, the knockout strains used in this study did not exhibit any significant differences (Supplementary Fig. 1). Each knockout strain was assessed for its effect on intracellular ligand retention and biosensor performance.

To assess the effect of efflux pump knockout on biosensor performance, a plasmid harboring the DmpR-GESS circuit was introduced into each knockout strain, and three phenolic ligands—phenol, 2-aminophenol (2AP), and 4-nitrophenol (4NP)—were tested. In this experiment, the DmpR M52I mutant was employed, as it exhibits enhanced sensitivity and broad substrate specificity toward phenolic compounds, including phenol, 2AP, and 4NP, and is applicable to the detection of diverse enzymatic reactions [28, 45, 55, 56]. Upon treatment with phenol, 3 out of the 21 efflux pump knockout strains—Δ*hsrA*, Δ*mdtA*, and Δ*emrE*—exhibited increased fluorescence intensity compared to that of the wild-type *E. coli* BW25113 strain (Fig. 2A). Upon treatment with 2AP, the Δ*mdtA*, Δ*emrE*, and Δ*mdtG* strains exhibited enhanced responsiveness compared to that of the wild-type strain (Fig. 2C), whereas treatment with 4NP resulted in increased responsiveness in the Δ*mdtA* and Δ*mdtG* strains relative to that of the wild type (Fig. 2E).

For efflux pump knockout hosts that showed improved responses to each ligand, DmpR-GESS reactions were performed across a range of ligand concentrations (Fig. 2B, D, and F). In all cases of selected efflux pump deletions, fluorescence responses at low ligand concentrations were improved compared to those of the wild type. Notably, the LODs were significantly reduced, indicating enhanced detection performance over the native baseline configuration (Supplementary Table 4). In addition, the Δ*mdtA* strain consistently exhibited a higher signal-to-noise ratio across all three phenolic compounds

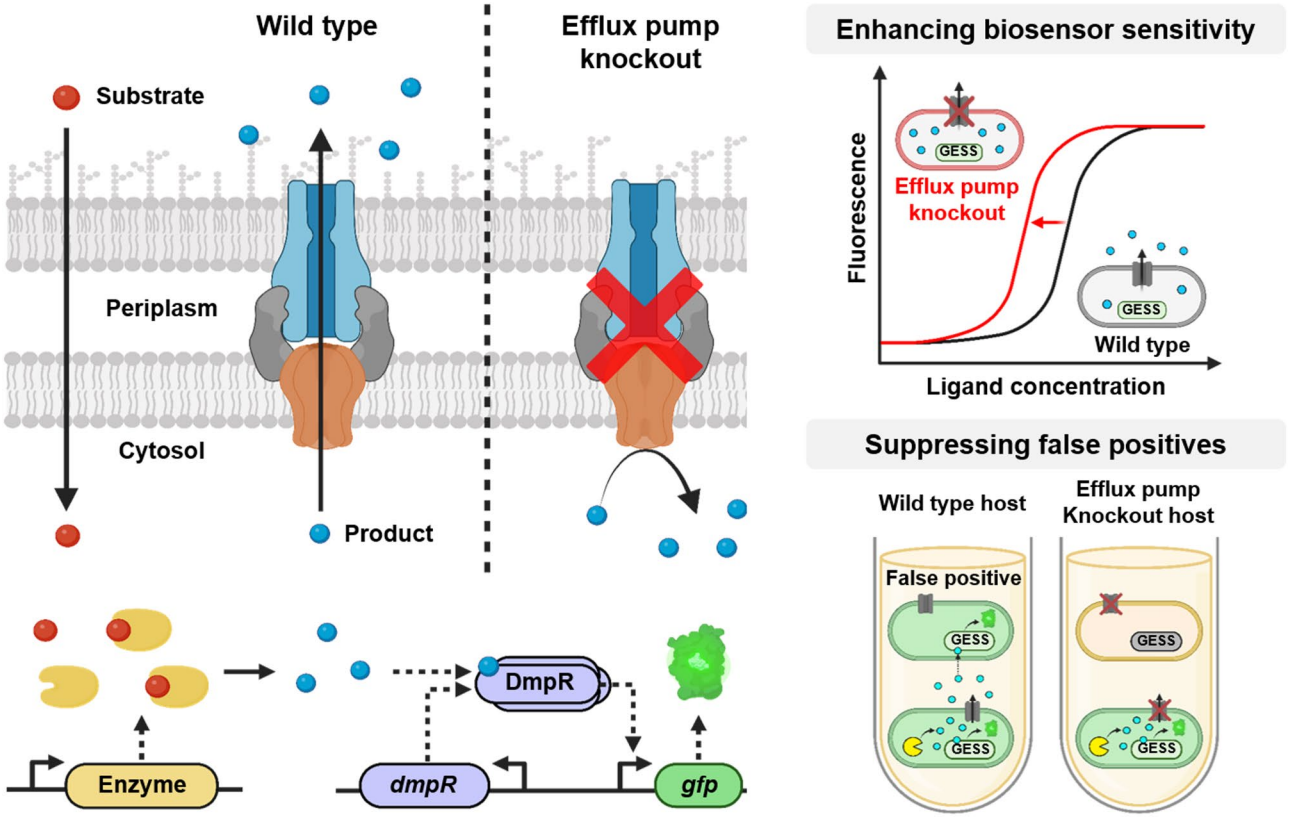


**Fig. 1** Schematic diagram of enhancing the performance of TF-based biosensor by efflux pump knockout. Deletion of the efflux pump can increase the intracellular concentration of products generated by enzymatic reactions, thereby affecting the sensitivity and precision of the TF-based biosensor. This ligand accumulation enables detection of ligands at lower concentrations. Furthermore, limiting intercellular ligand diffusion helps prevent false positives during single-cell screening

tested, suggesting its potential as a superior host chassis for biosensor applications.

In this study, knockout of *mdtA* enhanced the sensitivity of the biosensor to multiple phenolic compounds. To experimentally validate the effect of efflux pump knockout, intracellular and extracellular concentrations of phenolic compounds were analyzed by HPLC under identical ligand treatment conditions (Supplementary Fig. 2). When cultured with 100 μM phenolic substrate, the extracellular concentrations showed no significant differences between strains, whereas analysis of intracellular concentrations revealed that the efflux pump knockout strains exhibited relatively higher intracellular levels of phenolic compounds compared to the wild-type strain. Although the difference in intracellular phenol levels was modest, in the case of mutant DmpR-GESS (M52I), which is capable of detecting trace amounts of phenolic compounds, this difference is considered significant [45].

The role of efflux pumps in determining cellular ligand levels was confirmed, and experiments were conducted to modulate this by increasing efflux pump expression (Supplementary Fig. 3A). Based on the previous knockout experiments, two genes—*mdtA* and *mdtG*—were selected for additional expression and analysis in response to 4NP. DmpR-GESS plasmids containing additional efflux pump expression cassettes were introduced into BW25113, and fluorescence responses were measured after treatment with various concentrations of 4NP. Δ*mdtA* exhibited a significantly increased dynamic range, whereas additional expression of MdtA slightly reduced the signal (Supplementary Fig. 3B). In contrast, experiments targeting *mdtG* showed significant changes in both the gene knockout strain and the strain expressing additional MdtG (Supplementary Fig. 3C). These results collectively demonstrate that efflux pumps can modulate intracellular ligand levels through either deletion or overexpression, thereby enabling control over biosensor sensitivity.

### Biosensor-enhanced enzyme activity detection via efflux pump deletion

TF-based biosensors can be applied to enzyme engineering or discovery. To investigate whether efflux pump knockout also affects biosensor performance in the context of enzymatic reactions, we tested its effect using model enzymes. First, TPL, which catalyzes the

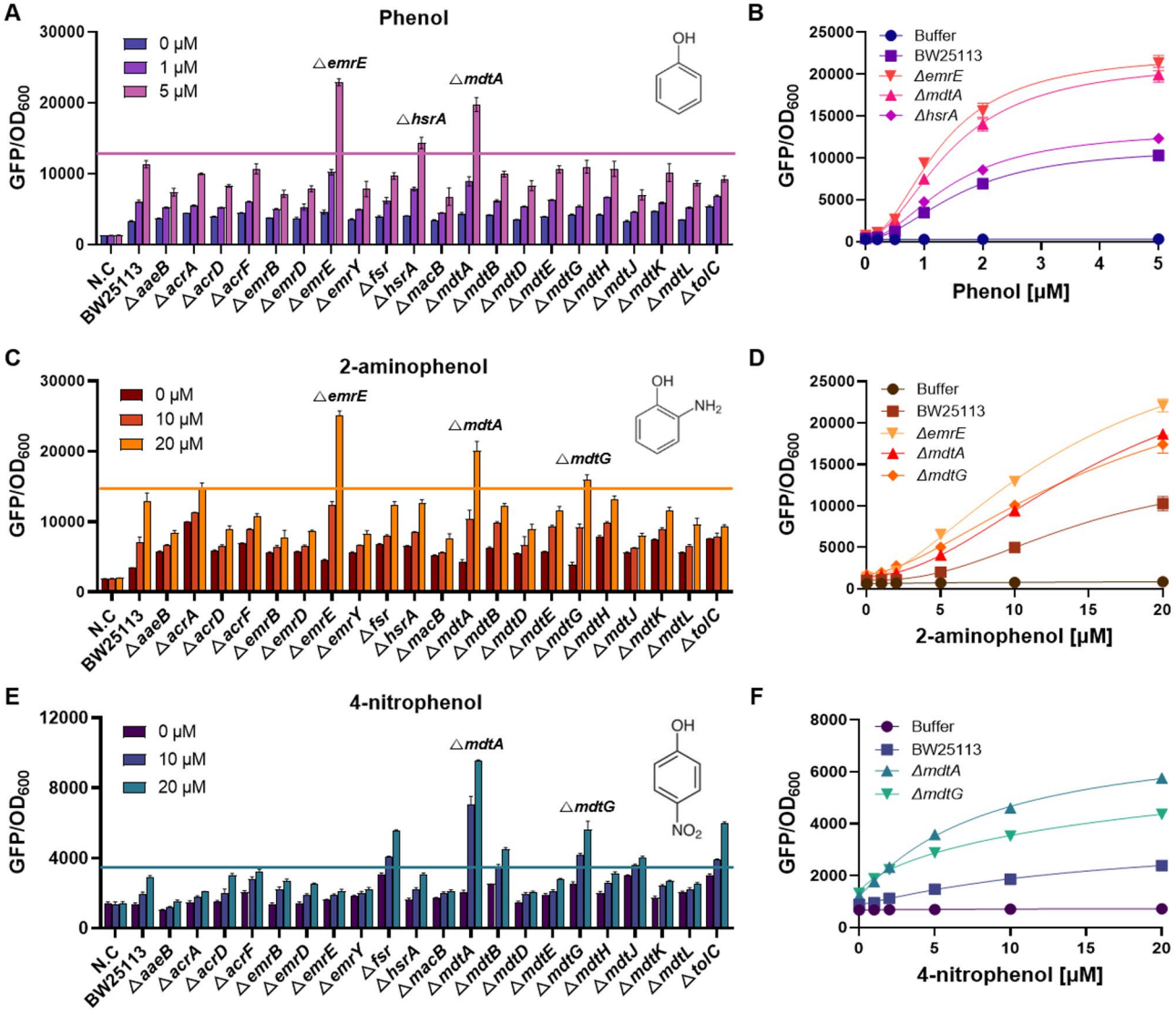


**Fig. 2** Fluorescence response of DmpR-GESS to phenolic compounds in efflux pump knockout strains. (**A**) Fluorescence response to phenol in efflux pump knockout strains. (**B**) Quantitative analysis of fluorescence intensities measured at varying concentrations of phenol. (**C**) Fluorescence response to 2AP in efflux pump knockout strains. (**D**) Quantitative analysis of fluorescence intensities measured at varying concentrations of 2AP. (**E**) Fluorescence response to 4NP in efflux pump knockout strains. (**F**) Quantitative analysis of fluorescence intensities measured at varying concentrations of 4NP. The data represent mean values from experiments conducted in triplicate ($n = 3$), and the error bars indicate standard deviations

conversion of L-tyrosine into phenol, was targeted (Fig. 3A, top) [41]. This experiment was conducted using three efflux pump knockout strains—Δ*mdtA*, Δ*emrE*, and Δ*hsrA*—that showed high fold changes in response to phenol. Upon treatment with 1 mM L-tyrosine, both Δ*mdtA* (4.05-fold) and Δ*emrE* (4.88-fold) exhibited higher fluorescence fold changes than the wild-type strain (3.05-fold) (Fig. 3A, bottom).

Second, PGA activity was evaluated. To facilitate detection of PGA activity by DmpR-GESS, we designed a synthetic substrate, HPPA, in which the β-lactam ring part was substituted with a phenolic moiety (Supplementary Fig. 4). Hydrolysis of HPPA by PGA yielded 2AP, a phenolic compound that activates DmpR (Fig. 3B, top). Following treatment with 50 μM HPPA, the Δ*mdtA* (18.99-fold) and Δ*emrE* (19.42-fold) strains showed markedly higher fluorescence fold changes than the wild-type strain (9.15-fold), indicating enhanced biosensor responses (Fig. 3B, bottom).

Finally, cellulase activity was evaluated using 4-nitrophenyl β-D-cellobioside ($4NPG_2$) as a substrate, which yields 4NP as the product (Fig. 3C, top). The assay was conducted using two efflux pump knockout strains, Δ*mdtA* and Δ*mdtG*, which previously showed improved biosensor performance with 4NP. Upon treatment with 400 μM $4NPG_2$, the Δ*mdtA* strain exhibited a higher fold change (2.58-fold) than the wild type (1.92-fold) (Fig. 3C, bottom). These results demonstrate that efflux pump

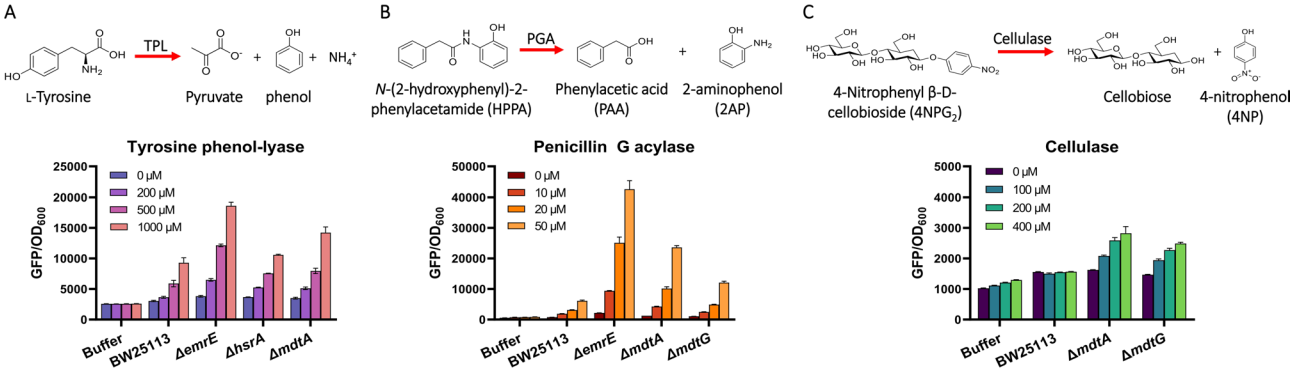


**Fig. 3** DmpR-GESS activation by target enzyme activity in efflux pump knockout strains. (A) Enzymatic reaction of TPL, which degrades L-tyrosine (top), and the DmpR-GESS response depending on the concentration of L-tyrosine (bottom). (B) Enzymatic reaction of PGA, which degrades HPPA (top), and the DmpR-GESS response depending on the concentration of HPPA (bottom). (C) Enzymatic reaction of cellulase, which degrades $4NPG_2$ (top), and the DmpR-GESS response depending on the concentration of $4NPG_2$ (bottom). Each data point represents the mean of three replicates (n=3), with error bars indicating standard deviations

knockout strains not only improve ligand detection but can also enhance the sensitivity of biosensor-based enzyme activity assays. Moreover, the Δ*mdtA* strain consistently exhibited higher fluorescence fold changes than the wild type across all tested substrates, suggesting its broad utility as an enhanced host chassis for enzyme activity screening.

### Suppressing false positives in single-cell enzyme screening

Efflux pump knockout can improve biosensor performance by preventing the diffusion of phenolic compounds—the ligands of DmpR—out of the cell. This strategy can also help reduce false positives in enzyme screening applications. As a whole-cell biosensor, *E. coli* BW25113, in which *bglA* was replaced with the DmpR-GESS circuit [26], was employed, and PGA was used as the model enzyme. To achieve both overexpression of the target enzyme and activation of DmpR-GESS driven by the σ54-dependent promoter, this study employed a two-step process that separates the growth and enzyme expression stage from the reaction stage [32]. Upon treating PGA-expressing cells with HPPA and performing FACS analysis during the second reaction step, it was found that at least 2 h of reaction time was required to obtain a signal distinguishable from that at the 0-h time point (Supplementary Fig. 5).

We conducted an experiment to identify false positives by monitoring GFP expression resulting from enzymatic reactions and constitutive red fluorescence protein (RFP) expression in negative cells (Fig. 4A). Negative cells, lacking enzyme activity, were designed to constitutively express RFP to allow differentiation from positive cells (Fig. 4D and G). In positive cells, the ligand produced by enzymatic activity activated the DmpR-GESS circuit, resulting in GFP expression (Fig. 4D and H). Although GFP accumulated within the positive cells, the enzymatic product could diffuse into neighboring cells via the cellular export system. Diffusion of 2AP produced by PGA into neighboring positive cells ($GFP^+$) activated the GESS circuit in negative cells ($RFP^+$), resulting in false positives ($GFP^+RFP^+$).

To investigate the impact of efflux pump deletion on reducing false positives, a mock library was constructed and analyzed in wild-type BW25113 and the *mdtA* knockout host. Through FACS analysis, cells were distinguished based on GFP and RFP signals, and the threshold GFP value for defining positive cells was determined according to the LOQ [46]. The proportion of false positives ($GFP^+RFP^+$) among the positive cells was markedly lower in the Δ*mdtA* host (Fig. 4B, F and I). In the BW25113 host, 74% of positive cells were false positives, whereas in the Δ*mdtA* host this proportion was reduced to less than 6%.

In FACS-based screening, cell sorting is typically performed by gating the top fraction of cells with the highest fluorescence signals. Considering this, the true positive ratio was calculated according to the proportion of high-GFP cells. Among the top 1% of cells with the highest GFP intensity, the true positive ratio was only 42% in wild-type BW25113, but increased to 94% in the Δ*mdtA* host (Fig. 4C). When the sorting window was expanded to the top 5% of GFP-expressing cells, the false positive rate exceeded 50% in the wild-type host but remained below 10% in the Δ*mdtA* host. These results demonstrate that the impact of efflux pump deletion on suppressing false positives and enhancing biosensor precision becomes more pronounced as the GFP sorting window is expanded.

### Engineering and characterization of PGA

Following the improvement of the PGA screening system through efflux pump regulation, enzyme engineering of *E. coli*-derived PGA was performed using the optimized platform (Fig. 5A). Based on the aforementioned results,

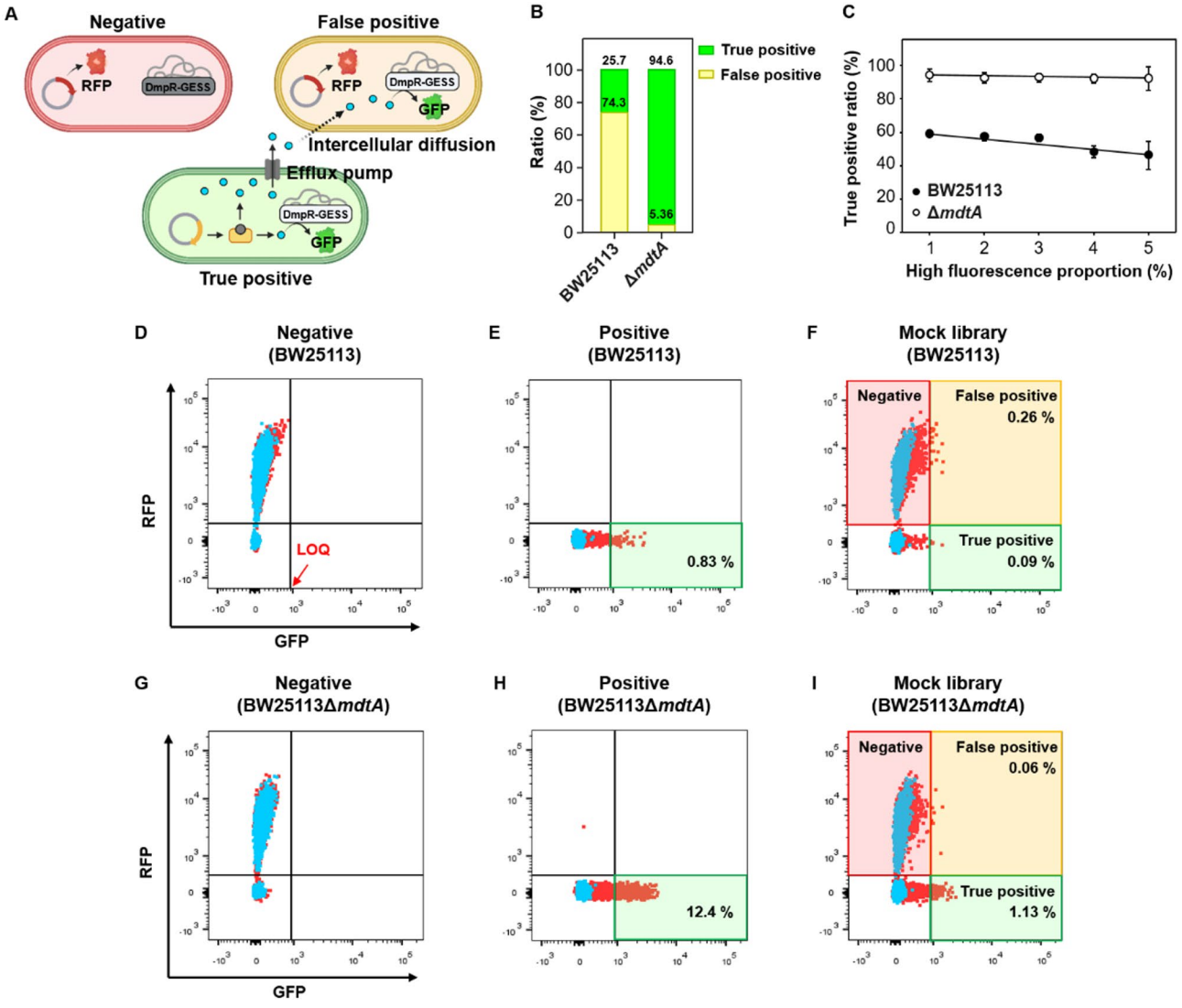


**Fig. 4** Analysis of mock library in wild-type and *mdtA* knockout strain. (**A**) Schematic illustration of false positives caused by intercellular ligand diffusion. Due to the diffusion of 2-aminophenol produced by PGA in neighboring positive cells, the GESS circuit in the negative cells can be activated, leading to GFP expression (false positive). (**B**) Relative ratio of true and false positives in BW25113 wild-type and Δ*mdtA* strains. (**C**) Analysis of true positive ratio according to the proportion of GFP-high cells. (**D**) Fluorescence analysis of negative cells expressing RFP in the wild-type strain. (**E**) Fluorescence analysis of positive cells expressing PGA and exhibiting GFP fluorescence by DmpR-GESS circuit in the wild-type strain. (**F**) Fluorescence analysis of a mock library containing a 1:1 mixture of positive and negative cells in the wild-type strain. (**G**) Fluorescence analysis of negative cells in BW25113 Δ*mdtA*. (**H**) Fluorescence analysis of positive cells in BW25113 Δ*mdtA*. (**I**) Fluorescence analysis of a mock library in BW25113 Δ*mdtA*. These data represent fluorescence profiles following treatment with 100 μM HPPA, comparing signals at 0 h (blue) and after 2 h of incubation (red)

cell sorting was conducted after a 2-h reaction. Three rounds of FACS were carried out, and the top 1% GFP signal cells in the third round were collected from the mutant library (Fig. 5B). Subsequently, individual variants were analyzed using a 96-well plate fluorescence assay (Fig. 5C). Among these, mutant enzymes exhibiting a higher fold change than the wild-type enzyme were obtained. A total of six variants, including one double mutant, were identified through sequencing. Mutant enzymes were expressed in *E. coli* BL21, and protein expression analysis revealed that although overall solubility was low, the soluble expression yield of the target band was higher in the mutants than in the wild type (Supplementary Fig. 6).

A separate DmpR-GESS assay and kinetic analysis were performed for the six mutant PGA variants. In terms of biosensor response to HPPA, the m2 variant exhibited high activity even at low substrate concentrations (Fig. 6A). Additionally, the other variants showed higher fluorescence signals than the wild-type enzyme, indicating that they are likely to possess improved catalytic activity. In the subsequent kinetic analysis, the m2 mutant showed an improved $K_M$, resulting in an increased $k_{cat}/K_M$ value, while the other variants showed enhancements

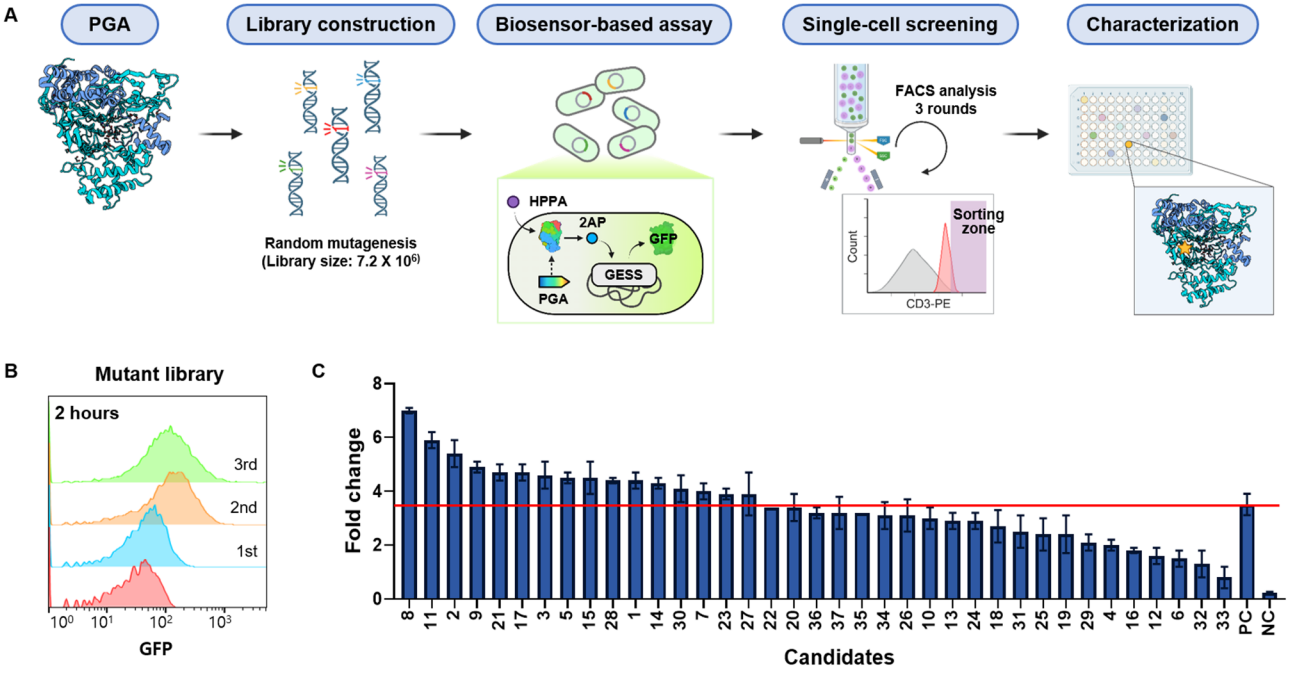


**Fig. 5** High-throughput screening of a PGA mutagenesis library using a biosensor-based FACS workflow. (**A**) Workflow for screening the PGA mutagenesis library using FACS. (**B**) Fluorescence analysis of the mutant library over three rounds of FACS sorting. (**C**) 96-well plate-based assay of sorted cells showing fold change in fluorescence. Fold change was calculated based on GFP/$OD_{600}$ values. Each data point represents the mean of two replicates ($n = 2$), with error bars indicating standard deviations

in turnover rate ($k_{cat}$) (Fig. 6B, Supplementary Fig. 7, and Table 1). Notably, the m11 (βM365T/βA456S) and m30 (βL277I) mutants exhibited substantially increased turnover rates of 96.2 $s^{-1}$ and 83.4 $s^{-1}$, respectively—up to threefold higher than that of the wild-type enzyme.

## Discussion

The performance of TF-based biosensors is typically enhanced by engineering individual genetic components, including promoters, TFs, and ribosome-binding sites [15, 29]. However, modifying the host that carries the genetic circuit offers an alternative strategy to enhance the performance of multiple biosensors simultaneously [18]. In this study, we focused on engineering membrane transport as a host-level strategy to control intracellular molecule concentration, thereby improving biosensor response and accuracy.

Efflux pumps associated with membrane transport are classified into families, such as the ATP-binding cassette (ABC) superfamily, major facilitator superfamily (MFS), and multidrug and toxic compound extrusion family, depending on their transport mechanisms and the types of compounds they export [12, 57–59]. Phenolic compounds, in particular, are often toxic to cells and are actively expelled by efflux pumps [33]. To improve the detection of phenolic compounds using DmpR-GESS, we evaluated biosensor performance across 21 *E. coli* strains, each with a single efflux pump gene knockout (Fig. 2). Four knockout strains—*mdtA*, *emrE*, *mdtG*, and *hsrA*—exhibited enhanced fluorescence responses to three phenolic compounds (phenol, 2AP, 4NP), with the Δ*mdtA* strain demonstrating consistent improvement across all three. Although the effect of the efflux pump knockout differs depending on the type of ligand, evaluation of biosensor functional parameters confirmed that both the LOD and dynamic range were improved compared with the wild-type strain (Supplementary Table 4). These results indicate that the knockout of the four efflux pump proteins led to an increase in intracellular phenolic compound concentration, which in turn enhanced the responsiveness of the biosensor. Although MdtABC, which includes MdtA, is known to be involved in the transport of phenolic compounds [33], this study demonstrated that other transporters—specifically EmrE from the SMR family, MdtG from the MFS family, and HsrA as a putative transporter—may also be involved in the transport of phenolic compounds.

Controlling intracellular ligand concentrations offers a practical strategy for tuning the sensitivity of TF-based biosensors, thereby enabling the adjustment of the activation threshold of the biosensors [18, 21] and allowing for a range of dynamic responses [14, 23, 60]. In general, biosensors with high sensitivity are advantageous for enzyme screening [22, 29]. However, in cases where a biosensor with reduced sensitivity is required—such as when attempting to further enhance the activity of an

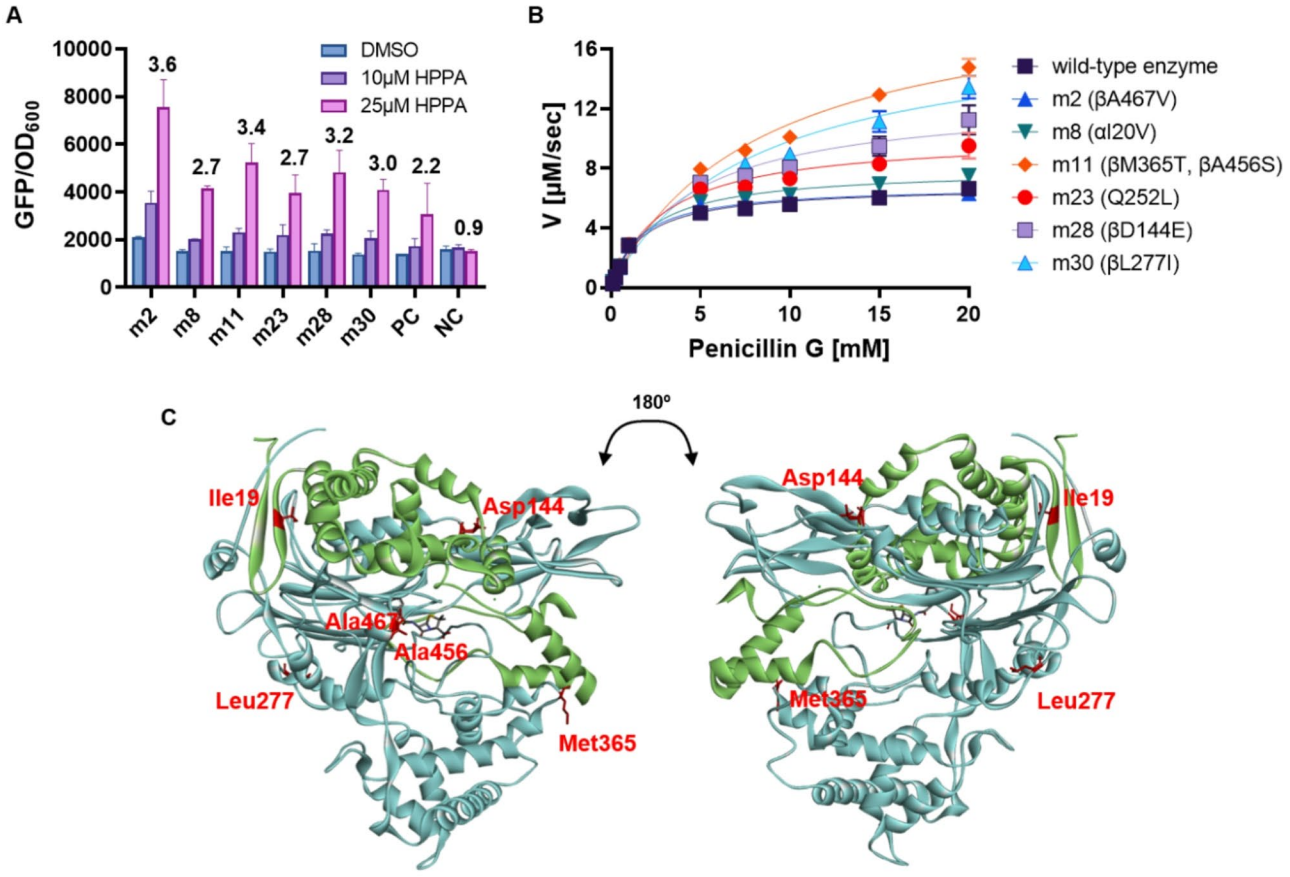


**Fig. 6** Characterization of mutant PGAs. (**A**) DmpR-GESS response across different concentrations of HPPA and corresponding fold-change values. (**B**) Michaelis–Menten curves comparing the wild-type and mutant PGAs. Each data point represents the mean of three replicates ($n=3$), with error bars indicating standard deviations. (**C**) PGA structure (PDB ID: 1GM7) presented with mutated residues of selected variants (**A** subunit in green; **B** subunit in cyan; mutated residues in red)

**Table 1** Kinetic parameters of wild-type and mutant PGAs

| | Wild type | m2 | m8 | m11 | m23 | m28 | m30 |
|---|---|---|---|---|---|---|---|
| **Mutation** | **-** | **βA467V** | **αI20V** | **βM365T, βA456S** | **Q252L** | **βD144E** | **βL277I** |
| $V_{max}$ (uM/sec) | 6.81 ± 0.49 | 6.82 ± 0.39 | 7.94 ± 0.53 | 20.2 ± 4.19 | 10.2 ± 1.31 | 12.7 ± 2.43 | 17.5 ± 4.95 |
| $K_M$ (mM) | 1.77 ± 0.59 | 1.62 ± 0.42 | 2.13 ± 0.61 | 8.38 ± 4.14 | 3.05 ± 1.51 | 4.52 ± 2.77 | 7.85 ± 5.48 |
| $k_{cat}$ ($s^{-1}$) | 32.4 ± 2.34 | 32.5 ± 1.86 | 37.8 ± 2.50 | 96.0 ± 20.0 | 48.4 ± 6.26 | 60.6 ± 11.6 | 83.4 ± 23.6 |
| $k_{cat}/K_M$ ($s^{-1}M^{-1}$) | 18.4 × $10^3$ | 20.1 × $10^3$ | 17.7 × $10^3$ | 11.5 × $10^3$ | 15.9 × $10^3$ | 13.4 × $10^3$ | 10.6 × $10^3$ |

* All kinetic parameters were calculated from triplicate measurements ($n=3$)

already highly active enzyme—the expression of additional efflux pumps can facilitate the selection of variants with the desired level of activity (Supplementary Fig. 3A). This approach enables the expansion of the dynamic range of the biosensor system to accommodate different stages of enzyme evolution, facilitating more precise screening under conditions that match the targeted improvement goals.

The effects of efflux pump knockout and additional expression varied depending on which efflux pump protein was modified. While knockout of *mdtA* showed a significant effect, its additional expression did not result in a substantial difference compared to that of the wild type, which is related to the function of MdtA. MdtA belongs to the resistance-nodulation-division family [2, 57, 61] and functions as part of a multicomponent complex, forming the MdtABC-TolC complex. In this complex, MdtB and MdtC span the inner membrane, TolC the outer membrane, and MdtA acts as a periplasmic adaptor connecting the components [62, 63]. Therefore, knocking out *mdtA* disrupts the function of the complex, whereas merely overexpressing *mdtA* gene does not lead to the formation of additional efflux pumps. In contrast, MdtG exhibited a relatively significant difference upon additional expression (Supplementary Fig. 3B and C). As MdtG belongs to the MFS family [64], it is presumed

to function as a monomer or possibly a homodimer [2]. Thus, overexpression of *mdtG* gene alone can effectively enhance cellular exportation. As the effects of knockout or additional expression vary depending on the characteristics of each efflux pump, considering these factors enables the customization of TF-based biosensors to meet diverse application needs.

To apply the efflux pump deletion strategy for biosensor-based detection of enzyme activity, three target enzymes—TPL, PGA, and cellulase—were tested along with their corresponding substrates: L-tyrosine, HPPA, and $4NPG_2$, respectively (Fig. 3). Each enzyme-substrate reaction produces one of the previously tested phenolic compounds—phenol, 2AP, or 4NP—which subsequently activate the DmpR-GESS circuit. In each case, the efflux pump knockout strains yielded stronger biosensor signals than the wild type, demonstrating a clear advantage in detecting enzymatic activity. In the case of Δ*emrE*, the largest effect was observed in the hydrolysis of HPPA by PGA, resulting in up to a 19-fold increase in normalized fluorescence, which was significantly higher than that observed in other strains (Fig. 3B, Δ*emrE*). This result indicates that efflux pump deletion not only improves the intracellular concentration of enzymatic products but may also influence substrate accumulation, leading to a more sensitive detection of enzyme activity. Furthermore, efflux pump knockout constitutes a host-level modification rather than an alteration of individual genetic circuits, providing a versatile strategy that can be applied not only to DmpR-GESS but also to pre-existing genetic circuits through simple implementation.

Notably, among the three enzyme reactions tested, cellulase exhibited relatively minor improvements. This can be interpreted in terms of the responsiveness of DmpR-GESS and the size of the substrate. Regarding the ligand specificity of DmpR M52I, 4NP exhibited lower fluorescence intensity compared with phenol and 2AP (Fig. 2) [45]. Therefore, the cellulase reaction, which generates 4NP, exhibited lower fluorescence intensity compared with the other enzyme reactions. Another contributing factor is the molecular size of the substrate. The performance of the whole-cell biosensor is inevitably influenced by host physiology, and larger substrates are less likely to enter the cell efficiently. In this case, limitations in substrate uptake, rather than intracellular accumulation of phenolic products, appear to play a greater role in constraining biosensor performance. To address this limitation, future strategies could complement efflux pump modulation with the engineering or co-expression of influx-related transporters, thereby facilitating substrate entry and further enhancing biosensor sensitivity [18, 20, 65].

Efflux pump knockout also provides practical advantages in flow cytometry screening by reducing false positives (Fig. 4). In such screenings, ligand diffusion between cells can cause non-expressing cells to exhibit fluorescence, leading to misidentification [27]. This issue is particularly critical in high-throughput screening, where only a few beneficial variants must be selected from a large library. By knocking out efflux pumps, enzymatic products are retained within positive cells, reducing false positive risk and significantly improving the efficiency of cell enrichment using FACS. Ultimately, this enhances both the sensitivity and precision of biosensor-based selection. In this study, experiments were conducted using DmpR-GESS; however, the false positive reduction achieved through efflux pump knockout could be broadly applicable to whole-cell biosensors.

The mutant enzymes obtained from enzyme engineering of PGA were subjected to GESS reaction using HPPA and activity assay using penicillin G (Fig. 6A). Mutant m2 exhibited higher apparent activity to low concentrations of HPPA than the wild-type and other mutant enzymes and showed the lowest $K_M$ value in the kinetics analysis (Table 1). Other mutants displayed up to a threefold increase in turnover rate relative to that of the wild type. The increased turnover rate may translate into enhanced enzymatic performance in vivo. In the cellular environment, where the intracellular space is highly confined and molecular crowding can lead to relatively high local substrate concentrations, enzymes with elevated turnover rates are more likely to operate near their maximal catalytic velocity [66, 67].

Structural analysis of the mutant PGA variants was performed using AlphaFold 3 [49] and CB-Dock2 [51]. In these mutants, most substitutions were located in the B subunit, with one found in the A subunit and another in the spacer peptide. The double mutant contained two mutations, βM365T and βA456S, both placed relatively close to the substrate entrance, suggesting potential structural implications for catalytic function (Fig. 6C). Notably, the substrate-binding cavity of the double mutant was predicted by CB-Dock2 to be relatively large, exceeding 1000 $Å^3$ (Supplementary Fig. 8). This finding suggests enhanced substrate accessibility in this variant and provides a structural explanation for the increased catalytic activity. Further analysis of the mutation sites and surrounding residues suggested that the substituted residues formed one to two additional interactions compared to the wild type (Supplementary Fig. 9).

The efflux pump knockout strategy validated in this study can be applied at the host level without the need to modify specific genetic circuits, offering substantial potential for broad utilization across various whole-cell biosensors. In particular, its ability to reduce false positives and improve both detection limits and precision makes it highly valuable for large-scale enzyme screening. However, the effects of this strategy may vary

depending on the specific ligand or host. Therefore, additional validation is required under conditions beyond phenolic compounds and the *E. coli* host. In future studies, this efflux pump strategy could be extended to other TF-based biosensors, providing a generalizable approach for enzyme development using biosensor platforms.

## Conclusion

This study proposes the regulation of efflux pumps as a host engineering strategy to enhance the performance of TF-based microbial biosensors by physically controlling the intracellular ligand concentration. In particular, knockout of several efflux pump genes, including *mdtA*, effectively increased the sensitivity of the biosensor toward phenolic ligands. This strategy was also applicable to the detection of the activities of enzymes that produce phenolic compounds as reaction products. Such an approach not only improves biosensor response but also suppresses intercellular diffusion of ligands, thereby reducing false positives and enabling reliable screening in high-throughput settings. Overall, host system engineering strategies—such as targeting efflux pumps—offer a broadly applicable approach to simultaneously enhance the sensitivity, precision, and efficiency of biosensor-based enzyme screening platforms.

### Abbreviations

| | |
|---|---|
| TF | Transcription factor |
| GESS | Genetic Enzyme Screening System |
| IPTG | Isopropyl β-D-1-thiogalactopyranoside |
| 2AP | 2-aminophenol |
| 4NP | 4-nitrophenol |
| PGA | Escherichia coli-driven) penicillin G acylase |
| HPPA | N-(2-hydroxyphenyl)-2-phenylacetamide |
| TPL | Tyrosine phenol-lyase |
| $4NPG_2$ | 4-nitrophenyl β-D-cellobioside |
| HPLC | High performance liquid chromatography |
| FACS | Fluorescence-activated cell sorting |
| GFP | Green fluorescent protein |
| RFP | Red fluorescent protein |

## Supplementary Information

The online version contains supplementary material available at https://doi.org/10.1186/s13036-025-00574-0.

Supplementary Material 1

### Acknowledgements

We thank the members of the Synthetic Biology Research Group at KRIBB for comments that greatly improved the manuscript. We also acknowledge the contribution of Dr. Victor de Lorenzo at the Center for National Biotechnology, CSIC, Madrid, Spain, for supplying the pSEVA plasmids.

### Author contributions

J.L. and B.Y. designed and conducted experiments, analyzed data, and wrote the manuscript. E.J. and H.K. conducted FACS experiments. E.R. and H.K. constructed DmpR-GESS genetic circuits. J.S., H.L., and D.H.L. assisted in experimental design and manuscript revision. K.K.K. and S.G.L. conceptualized and supervised the study and critically revised the manuscript. K.K.K. and S.G.L. are corresponding authors and supervised all aspects of the research. All authors read and approved the final manuscript.

### Funding

This work was supported by the Bio & Medical Technology Development Program (grant numbers: RS-2021-NR056563, RS-2024-00445145, RS-2024-00508861) of the National Research Foundation, the National Research Council of Science & Technology grant (No. CAP20024-200), funded by the Korean government (MSIT), and by the Korea Research Institute of Bioscience and Biotechnology (KRIBB) Research Initiative Program (KGM1302511).

### Data availability

No datasets were generated or analysed during the current study.

## Declarations

### Ethics approval and consent to participate

Not applicable.

### Consent for publication

Not applicable.

### Competing interests

The authors declare no competing interests.

### Author details

[1]Synthetic Biology Research Center, Korea Research Institute of Bioscience and Biotechnology (KRIBB), Daejeon 34141, Republic of Korea
[2]Korea Biofoundry, Korea Research Institute of Bioscience and Biotechnology (KRIBB), Daejeon 34141, Republic of Korea
[3]Department of Biosystems and Bioengineering, KRIBB School of Biotechnology, University of Science and Technology (UST), Daejeon 34113, Republic of Korea
[4]Graduate School of Engineering Biology, Korea Advanced Institute of Science and Technology (KAIST), Daejeon 34141, Republic of Korea
[5]Department of Integrative Biotechnology, College of Biotechnology and Bioengineering, Sungkyunkwan University, Suwon 16419, Republic of Korea

Received: 5 August 2025 / Accepted: 18 October 2025
Published online: 12 November 2025

### References

1. Nikaido H. Multidrug efflux pumps of gram-negative bacteria. J Bacteriol. 1996;178(20):5853–9.
2. Du D, Wang-Kan X, Neuberger A, van Veen HW, Pos KM, Piddock LJV, et al. Multidrug efflux pumps: structure, function and regulation. Nat Rev Microbiol. 2018;16(9):523–39.
3. Du D, Wang Z, James NR, Voss JE, Klimont E, Ohene-Agyei T, et al. Structure of the AcrAB-TolC multidrug efflux pump. Nature. 2014;509(7501):512–5.
4. Zwama M, Yamaguchi A. Molecular mechanisms of AcrB-mediated multidrug export. Res Microbiol. 2018;169(7–8):372–83.
5. Zwama M, Yamasaki S, Nakashima R, Sakurai K, Nishino K, Yamaguchi A. Multiple entry pathways within the efflux transporter AcrB contribute to multidrug recognition. Nat Commun. 2018;9(1):124.
6. Orelle C, Mathieu K, Jault JM. Multidrug ABC transporters in bacteria. Res Microbiol. 2019;170(8):381–91.
7. Bogomolnaya LM, Andrews KD, Talamantes M, Maple A, Ragoza Y, Vazquez-Torres A, et al. The ABC-type efflux pump macab protects Salmonella enterica serovar typhimurium from oxidative stress. MBio. 2013;4(6):e00630–13.
8. Pasqua M, Grossi M, Zennaro A, Fanelli G, Micheli G, Barras F, et al. The varied role of efflux pumps of the MFS family in the interplay of bacteria with animal and plant cells. Microorganisms. 2019;7(9):285.
9. Okusu H, Ma D, Nikaido H. AcrAB efflux pump plays a major role in the antibiotic resistance phenotype of Escherichia coli multiple-antibiotic-resistance (Mar) mutants. J Bacteriol. 1996;178(1):306–8.
10. Sulavik MC, Houseweart C, Cramer C, Jiwani N, Murgolo N, Greene J, et al. Antibiotic susceptibility profiles of Escherichia coli strains lacking multidrug efflux pump genes. Antimicrob Agents Chemother. 2001;45(4):1126–36.

11. Piddock LJ. Clinically relevant chromosomally encoded multidrug resistance efflux pumps in bacteria. Clin Microbiol Rev. 2006;19(2):382–402.
12. Gaurav A, Bakht P, Saini M, Pandey S, Pathania R. Role of bacterial efflux pumps in antibiotic resistance, virulence, and strategies to discover novel efflux pump inhibitors. Microbiology. 2023;169(5):001333.
13. Wang W, Guo Q, Xu X, Sheng ZK, Ye X, Wang M. High-level Tetracycline resistance mediated by efflux pumps Tet(A) and Tet(A)-1 with two start codons. J Med Microbiol. 2014;63(11):1454–9.
14. Diao J, Charlebois DA, Nevozhay D, Bodi Z, Pal C, Balazsi G. Efflux pump control alters synthetic gene circuit function. ACS Synth Biol. 2016;5(7):619–31.
15. Chen Y, Ho JML, Shis DL, Gupta C, Long J, Wagner DS, et al. Tuning the dynamic range of bacterial promoters regulated by ligand-inducible transcription factors. Nat Commun. 2018;9(1):64.
16. Kasey CM, Zerrad M, Li Y, Cropp TA, Williams GJ. Development of transcription Factor-Based designer macrolide biosensors for metabolic engineering and synthetic biology. ACS Synth Biol. 2018;7(1):227–39.
17. Rogers JK, Guzman CD, Taylor ND, Raman S, Anderson K, Church GM. Synthetic biosensors for precise gene control and real-time monitoring of metabolites. Nucleic Acids Res. 2015;43(15):7648–60.
18. Miyake R, Ling H, Foo JL, Fugono N, Chang MW. Transporter-Driven engineering of a genetic biosensor for the detection and production of Short-Branched chain fatty acids in Saccharomyces cerevisiae. Front Bioeng Biotechnol. 2022;10:838732.
19. Lu M, Sha Y, Kumar V, Xu Z, Zhai R, Jin M. Transcription factor-based biosensor: A molecular-guided approach for advanced biofuel synthesis. Biotechnol Adv. 2024;72:108339.
20. Berepiki A, Kent R, Machado LFM, Dixon N. Development of High-Performance whole cell biosensors aided by statistical modeling. ACS Synth Biol. 2020;9(3):576–89.
21. Zhang X, He Y, Wu Z, Liu G, Tao Y, Jin JM, et al. Whole-Cell biosensors aid exploration of Vanillin transmembrane transport. J Agric Food Chem. 2021;69(10):3114–23.
22. Chouichit P, Whangsuk W, Sallabhan R, Mongkolsuk S, Loprasert S. A highly sensitive biosensor with a single-copy evolved sensing cassette for Chlorpyrifos pesticide detection. Microbiol (Reading). 2020;166(11):1019–24.
23. La Fleur LC, Zhang Z, McRoberts-Amador C, Christopher J, Reed M, Zheng J, et al. Directed evolution of a Macrolide-Sensing transcription factor biosensor for the detection of macrolactone aglycones via effector walking and efflux pump deletion. Biochemistry. 2025;64(7):1560–71.
24. Adam GC, Meng J, Rizzo JM, Amoss A, Lusen JW, Patel A, et al. Use of high-throughput mass spectrometry to reduce false positives in protease uHTS screens. J Biomol Screen. 2015;20(2):212–22.
25. Singh D, Letter. Addressing false positives in high-throughput screening: a call for better predictive models. Assay Drug Dev Technol. 2025.
26. Yeom SJ, Kwon KK, An JU, Park SH, Lee JY, Rha E, et al. Single-Cell-Based screening and engineering of d-Amino acid amidohydrolases using artificial amidophenol substrates and microbial biosensors. J Agric Food Chem. 2022;70(4):1203–11.
27. Trivedi VD, Mohan K, Chappell TC, Mays ZJS, Nair NU. Cheating the cheater: suppressing False-Positive enrichment during Biosensor-Guided biocatalyst engineering. ACS Synth Biol. 2022;11(1):420–9.
28. Choi S-L, Rha E, Lee SJ, Kim H, Kwon G, Jeong Y-S, et al. Toward a generalized and High-throughput enzyme screening system based on artificial genetic circuits. ACS Synth Biol. 2014;3(3):163–71.
29. Yeom SJ, Kim M, Kwon KK, Fu Y, Rha E, Park SH, et al. A synthetic microbial biosensor for high-throughput screening of lactam biocatalysts. Nat Commun. 2018;9(1):5053.
30. Kim SK, Kim SH, Subhadra B, Woo S-G, Rha E, Kim S-W, et al. A genetically encoded biosensor for monitoring isoprene production in engineered Escherichia coli. ACS Synth Biol. 2018;7(10):2379–90.
31. Lee JY, Sung BH, Oh SH, Kwon KK, Lee H, Kim H, et al. C1 compound biosensors: Design, functional Study, and applications. Int J Mol Sci. 2019;20(9):2253.
32. Kwon KK, Yeom SJ, Choi SL, Rha E, Lee H, Kim H, et al. Acclimation of bacterial cell state for high-throughput enzyme engineering using a DmpR-dependent transcriptional activation system. Sci Rep. 2020;10(1):6091.
33. Sui X, Guo L, Bao Z, Xian M, Zhao G. Efflux pumps and porins enhance bacterial tolerance to phenolic compounds by inhibiting hydroxyl radical generation. Microorganisms. 2025;13(1):202.
34. Srirangan K, Orr V, Akawi L, Westbrook A, Moo-Young M, Chou CP. Biotechnological advances on penicillin G acylase: pharmaceutical implications, unique expression mechanism and production strategies. Biotechnol Adv. 2013;31(8):1319–32.
35. Kwon KK, Yeom S-J, Lee D-H, Jeong KJ, Lee S-G. Development of a novel cellulase biosensor that detects crystalline cellulose hydrolysis using a transcriptional regulator. Biochem Biophys Res Commun. 2018;495(1):1328–34.
36. Cobos-Purc L, Rodriguez-Herrera R, Cano-Cabrera JC, Aguayo-Morales H, Silba-Belmares SY, Gallegos ACF, et al. Classical and new pharmaceutical uses of bacterial penicillin G acylase. Curr Pharm Biotechnol. 2020;21(4):287–97.
37. Pan X, Xu L, Li Y, Wu S, Wu Y, Wei W. Strategies to improve the biosynthesis of beta-Lactam antibiotics by penicillin G acylase: progress and prospects. Front Bioeng Biotechnol. 2022;10:936487.
38. Baba T, Ara T, Hasegawa M, Takai Y, Okumura Y, Baba M, et al. Construction of Escherichia coli K-12 in-frame, single-gene knockout mutants: the Keio collection. Mol Syst Biol. 2006;2(1):2006–0008.
39. Karp PD, Paley S, Caspi R, Kothari A, Krummenacker M, Midford PE, Moore LR, Subhraveti P, Gama-Castro S, Tierrafria VH, Lara P, Muñiz-Rascado L, Bonavides-Martinez C, Santos-Zavaleta A, Mackie A, Sun G, Ahn-Horst TA, Choi H, Covert MW, Collado-Vides J, Paulsen I. The EcoCyc database (2023). EcoSal Plus. 2023;11:esp-0002-2023.
40. Cherepanov PP, Wackernagel W. Gene disruption in Escherichia coli: TcR and KmR cassettes with the option of Flp-catalyzed excision of the antibiotic-resistance determinant. Gene. 1995;158(1):9–14.
41. Barbolina MV, Phillips RS, Gollnick PD, Faleev NG, Demidkina TV. Citrobacter freundii tyrosine phenol-lyase: the role of asparagine 185 in modulating enzyme function through stabilization of a quinonoid intermediate. Protein Eng. 2000;13(3):207–15.
42. Ko KC, Han Y, Choi JH, Kim GJ, Lee SG, Song JJ. A novel bifunctional endo-/exo-type cellulase from an anaerobic ruminal bacterium. Appl Microbiol Biotechnol. 2011;89(5):1453–62.
43. Marešová H, Marková Z, Valešová R, Sklenář J, Kyslík P. Heterologous expression of leader-less Pga gene in Pichia pastoris: intracellular production of prokaryotic enzyme. BMC Biotechnol. 2010;10(1):7.
44. Rha E, Kim S, Choi SL, Hong SP, Sung MH, Song JJ, et al. Simultaneous improvement of catalytic activity and thermal stability of tyrosine phenol-lyase by directed evolution. FEBS J. 2009;276(21):6187–94.
45. Kim H, Seong W, Rha E, Lee H, Kim SK, Kwon KK, et al. Machine learning linked evolutionary biosensor array for highly sensitive and specific molecular identification. Biosens Bioelectron. 2020;170:112670.
46. Armbruster DA, Pry T. Limit of blank, limit of detection and limit of quantitation. Clin Biochem Rev. 2008;29(Suppl 1):S49.
47. Little TA. Method validation Essentials, limit of blank, limit of detection, and limit of quantitation. BioPharm Int. 2015;28(4).
48. Bradford MM. A rapid and sensitive method for the quantitation of microgram quantities of protein utilizing the principle of protein-dye binding. Anal Biochem. 1976;72(1–2):248–54.
49. Abramson J, Adler J, Dunger J, Evans R, Green T, Pritzel A, et al. Accurate structure prediction of biomolecular interactions with alphafold 3. Nature. 2024;630(8016):493–500.
50. Liu Y, Grimm M, Dai WT, Hou MC, Xiao ZX, Cao Y. CB-Dock: a web server for cavity detection-guided protein-ligand blind Docking. Acta Pharmacol Sin. 2020;41(1):138–44.
51. Liu Y, Yang X, Gan J, Chen S, Xiao ZX, Cao Y. CB-Dock2: improved protein-ligand blind Docking by integrating cavity detection, Docking and homologous template fitting. Nucleic Acids Res. 2022;50(W1):W159–64.
52. McVey CE, Walsh MA, Dodson GG, Wilson KS, Brannigan JA. Crystal structures of penicillin acylase enzyme-substrate complexes: structural insights into the catalytic mechanism. J Mol Biol. 2001;313(1):139–50.
53. Yang X, Liu Y, Gan J, Xiao ZX, Cao Y. FitDock: protein-ligand Docking by template fitting. Brief Bioinform. 2022;23(3):bbac087.
54. Yang NJ, Hinner MJ. Getting across the cell membrane: an overview for small molecules, peptides, and proteins. Methods Mol Biol. 2014:29–53.
55. Pavel H, Shingler MFV. An aromatic effector specificity mutant of the trasncriptional regulator DmpR overcomes the growth constraints of Pseudomonas sp. strain CF600 on para-substituted methylphenols. J Bacteriol. 1994;176(24):7550–7.
56. Wise AA, Kuske CR. Generation of novel bacterial regulatory proteins that detect priority pollutant phenols. Appl Environ Microbiol. 2000;66(1):163–9.
57. Teelucksingh T, Thompson LK, Cox G. The evolutionary conservation of Escherichia coli drug efflux pumps supports physiological functions. J Bacteriol. 2020;202(22):e00367–20.
58. Pao SS, Paulsen IT. Jr. MHS. Major facilitator superfamily. Microbiol Mol Biol Rev. 1998;62(1):1–34.

59. Shcherbakov AA, Hisao G, Mandala VS, Thomas NE, Soltani M, Salter EA, et al. Structure and dynamics of the drug-bound bacterial transporter EmrE in lipid bilayers. Nat Commun. 2021;12(1):172.
60. Hui CY, Liu MQ, Guo Y. Synthetic bacteria designed using Ars operons: a promising solution for Arsenic biosensing and bioremediation. World J Microbiol Biotechnol. 2024;40(6):192.
61. Nagakubo S, Nishino K, Hirata T, Yamaguchi A. The putative response regulator BaeR stimulates multidrug resistance of Escherichia coli via a novel multidrug exporter system, MdtABC. J Bacteriol. 2002;184(15):4161–7.
62. Zgurskaya HI, Krishnamoorthy G, Ntreh A, Lu S. Mechanism and function of the outer membrane channel TolC in multidrug resistance and physiology of Enterobacteria. Front Microbiol. 2011;2:189.
63. Poole K. Multidrug efflux pumps and antimicrobial resistance in Pseudomonas aeruginosa and related organisms. J Mol Microbiol Biotechnol. 2001;3(2):255–64.
64. Fabrega A, Martin RG, Rosner JL, Tavio MM, Vila J. Constitutive SoxS expression in a fluoroquinolone-resistant strain with a truncated SoxR protein and identification of a new member of the marA-soxS-rob regulon, MdtG. Antimicrob Agents Chemother. 2010;54(3):1218–25.
65. Oh SJ, An JU, Park JH, Choi EW, Kim SK, Woo SG, Kim TH, Sung BH, Lee SG, Kwon KK, Lee DH. A high-sensitivity genetically encoded biosensor for terephthalic acid detection in PET degradation. ACS Synth Biol. 2025;14(9):3497–509.
66. Bennett BD, Kimball EH, Gao M, Osterhout R, Van Dien SJ, Rabinowitz JD. Absolute metabolite concentrations and implied enzyme active site occupancy in Escherichia coli. Nat Chem Biol. 2009;5(8):593–9.
67. Ellis RJ. Macromolecular crowding: Obvious but underappreciated. Trends Biochem Sci. 2001;26(10):597–604.

## Publisher's note